Eur. Phys. J. D (2010)
DOI: 10.1140/epjd/e2010-00144-2

THE EUROPEAN PHYSICAL JOURNAL D

Regular Article

Spontaneous motion of localized structures and localized patterns induced by delayed feedback

M. Tlidi[1,a], A.G. Vladimirov[2], D. Turaev[3], G. Kozyreff[1], D. Pieroux[1], and T. Erneux[1]

[1] Optique Nonlinéaire Théorique, Université libre de Bruxelles (U.L.B.), CP 231, Campus Plaine, 1050 Bruxelles, Belgium
[2] Weierstrass Institute for Applied Analysis and Stochastics, Mohrenstrasse 39, 10117 Berlin, Germany
[3] Imperial College, London, UK

Received 26 November 2009 / Received in final form 8 April 2010
Published online 26 May 2010 –

Abstract. We study the properties of 2D dissipative structures in a coherently driven optical resonator subjected to a delayed feedback. It has been predicted that delayed feedback can lead to the spontaneous motion of bright localized structures [M. Tlidi et al., Phys. Rev. Lett. **103**, 103904 (2009)]. We study here the phenomenon in detail. In particular, we show that the delayed feedback induces a spontaneous motion of periodic patterns and dark localized structures. We focus our analysis on nascent optical bistability regime where the space time dynamics is described by a variational Swift-Hohenberg equation. In the absence of delayed feedback, dark localized structures and patterns do not move. This behavior occurs when the product of the delay time and the feedback strength exceeds some critical value.

1 Introduction

Dissipative localized structures (DLS) consist of bright or dark pulses in spatially extended systems. In optics, they are sometimes called cavity solitons, and belong to the class of dissipative structures found far from equilibrium [1–5]. They may either be isolated, randomly distributed or self-organized in clusters forming a well-defined spatial pattern. In two-dimensional (2D) settings, theoretical prediction of high degree of multistability between structures having different number of peaks was established for driven nonlinear planar cavities [6–11]. This prediction has been confirmed by experimental evidence of DLS in various nonlinear optical systems [12–27]. Transverse optical structures can be either stationary or not. The motion can be induced by the vorticity [28,29], by finite relaxation rates [30–32], phase gradient [33], so-called Ising-Bloch transition [34–36], by walk-off or convection or by the symmetry breaking due to off-axis feedback [37–41], or even by resonator detuning [42]. This subject is relatively well understood (see overviews on that issue [43–54]). So far, however, the inclusion of the delayed feedback in the dynamics of spatially extended systems is a relatively new area of research [55,56]. Recently, a model for the study of cavity solitons in broad area vertical-cavity surface-emitting lasers subjected to a frequency-selective feedback was proposed in [57,58]. Other studies of various spatially extended systems with time delay have motivated further to investigate this subject [59–62].

In this paper, we investigate the influence of the delayed feedback on the mobility of dark 2D dissipative localized structures and localized patterns. We consider a passive cavity filled with a two-level medium driven by a coherent injected beam. In addition, we introduce a time delayed feedback control via an external mirror. We restrict our analysis to the vicinity of the critical point associated with optical bistability and close to the pattern forming process. We first derive a delayed Swift-Hohenberg equation. Then we report on an instability leading to a spontaneous motion of dark dissipative localized structures. We show that when the product of the delay time and the feedback amplitude exceeds a certain threshold, dark dissipative localized structures and patterns start to move in an arbitrary direction. This completes the previous short note on the motion of bright 2D DLS where we have derived analytically the threshold as well as the velocity of these structures [63]. A similar analysis has been applied to moving fronts [64].

In the next section, we briefly introduce the model for passive nonlinear cavity with delayed feedback. The derivation of a delayed Swift-Hohenberg is presented in Section 3. The motion of periodic patterns under the effect of delayed feedback is presented in Section 4. Spontaneous motion of dissipative dark localized structures is presented in Section 5. Finally, we conclude in Section 6.

2 Passive nonlinear cavity with delayed feedback

In order to investigate the effect of delayed feedback on properties of the 2D transverse patterns, we consider a

[a] e-mail: mtlidi@ulb.ac.be

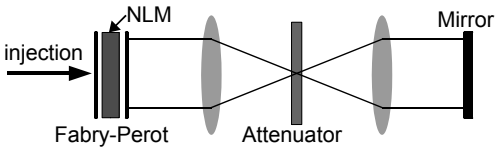

Fig. 1. Schematic setup of a Fabry-Perot cavity with delayed optical feedback and driven by a coherent external injected beam. The nonlinear medium (NLM) consists of two-level atoms. To control the feedback strength we use an attenuator and to compensate the diffraction in the external cavity we used two lenses.

Fabry-Perot cavity filled with two-level atoms without population inversion and driven by a coherent external injected beam. The delayed feedback is modeled by an external mirror located at a distance L from the right facet of the Fabry-Perot resonator as shown in Figure 1. The delayed feedback due to the presence of an external cavity is characterized by: (i) the time delay $\tilde{\tau} = 2L/c$ which is the round-trip time in the external cavity, where c is the speed of light and L is the length of the external cavity; (ii) the feedback strength $\tilde{\eta} = R(1-R_F^2)/(TR_F)$ proportional to the reflectivity of the external mirror R and inversely proportional to the Fabry-Perot round trip time T, R_F is the reflectivity of the laser cavity facets; and (iii) the phase $\phi = \omega_e\tilde{\tau}$ where ω_e is the frequency of the injected signal. We adopt the Lang-Kobayashi approach to model the delayed feedback [65]. This approach is based on two approximations: a single longitudinal mode operation and the reflected field is sufficiently attenuated that it can be modeled by a single delay term. More precisely, Lang and Kobayashi (LK) formulated two delay differential equations for an idealized case of a single mode semiconductor laser subject to optical feedback. In addition to the delayed feedback, we consider a paraxial approximation to describe diffraction in a plane orthogonal to propagation. We assume that the laser operates in a single longitudinal mode, and diffraction occurs only inside the Fabry-Perot cavity. Using a self-imaging technique, we can easily compensate the diffraction in the external cavity. Under these approximations, the driven passive nonlinear cavity can be described by the following delayed Maxwell-Bloch equations

$$\frac{\partial E(\tilde{\mathbf{r}},\tilde{t})}{\partial \tilde{t}} = \gamma_c[-(1+i\theta)E(\tilde{\mathbf{r}},\tilde{t}) - 2CP + E_i + ia\tilde{\nabla}^2 E(\tilde{\mathbf{r}},\tilde{t}) + \tilde{\eta}\exp(i\phi)[E(\tilde{\mathbf{r}},\tilde{t}-\tilde{\tau}) - E(\tilde{\mathbf{r}},\tilde{t})]] \quad (1)$$

$$\frac{\partial P}{\partial \tilde{t}} = \gamma_\perp[-(1+i\delta)P + E(\tilde{\mathbf{r}},\tilde{t})D] \quad (2)$$

$$\frac{\partial D}{\partial \tilde{t}} = \gamma_\parallel\left[1 - D - \frac{E^*(\tilde{\mathbf{r}},\tilde{t})P + E(\tilde{\mathbf{r}},\tilde{t})P^*}{2}\right] \quad (3)$$

where $E(\tilde{\mathbf{r}},\tilde{t})$ is the slowly varying envelope field with decay rate γ_c, E_i is the injected signal which is real and positive, $P = P(\tilde{\mathbf{r}},\tilde{t})$ and $D = D(\tilde{\mathbf{r}},\tilde{t})$ are the atomic polarization and population difference with decay rates $\gamma_\parallel$ and $\gamma_\perp$, respectively. $\theta = (\omega_c - \omega_e)/\gamma_c$ and $\delta = (\omega_a - \omega_e)/\gamma_\perp$, where ω_c, ω_a and ω_e are the cavity, atomic, and external field frequencies, respectively. The cooperativity parameter is denoted by C. The transverse Laplacian, which describes diffraction in the paraxial approximation, is given by $\tilde{\nabla}^2 = \partial^2_{\tilde{x}\tilde{x}} + \partial^2_{\tilde{y}\tilde{y}}$. The diffraction coefficient $a = 1/(4\pi T\mathcal{F})$ where $\mathcal{F} = S_\perp/(\Lambda_c L_c)$ is the Fresnel number with $S_\perp$ is the transverse area, Λ_c is the optical wavelength of the electric field, and L_c is the length of the Fabry-Perot cavity. It is convenient to subtract the cavity field $E(\tilde{\mathbf{r}},\tilde{t})$ from its delayed value $E(\tilde{\mathbf{r}},\tilde{t}-\tilde{\tau})$, so that when we put $\tilde{\tau} = 0$, we recover the homogeneous steady states of the system solutions of equations: $E_i = E_s[1 + i\theta + 2C(1+\delta^2)/(1+\delta^2+|E_s|^2)]$, $P_s = E_s D_s/(1+i\delta)$, and $D_s = (1+\delta^2)/(1+\delta^2+|E_s|^2)$. In the next section we perform the nonlinear analysis in the double limit of nascent optical bistability and close to the pattern forming threshold.

3 Derivation of the Swift-Hohenberg equation with delay

The aim of this section is to present the derivation of the Swift-Hohenberg with delay feedback. To do that, we explore the space time dynamics in the vicinity of the critical point associated with nascent bistability where $\partial E_i/\partial|E_s| = \partial^2 E_i/\partial|E_s|^2 = 0$. The coordinates of this point in the case of antisymmetric detuning ($\theta = -\delta$) are given by $E_c = (1+i\delta)\sqrt{3}$, $P_c = \sqrt{3}/4$, $D_c = 1/4$, $E_{ic} = 3(1+\delta^2)\sqrt{3}$, and $C_c = 4(1+\delta^2)$.

We seek corrections to the steady states at criticality that depend on time and space through the slow variables

$$t = \varepsilon^2\tilde{t}, \quad \text{and} \quad (x,y) = \left(\frac{\varepsilon}{a}\right)^{1/2}(\tilde{x},\tilde{y}) \quad (4)$$

and therefore $a\tilde{\nabla}^2 = \varepsilon\nabla^2$, where $\nabla^2 = \partial^2_{xx} + \partial^2_{yy}$. For the delay parameters we consider the following scaling

$$\tilde{\eta} = \eta\varepsilon^2, \quad \text{and} \quad \tilde{\tau} = \frac{\tau}{\varepsilon^2}. \quad (5)$$

Even for very small R the absolute value of the dimensionless product $|\eta\tau|$ can be made arbitrary large by taking the external cavity length much longer than the internal one, $\tau/T \gg 1$.

For mathematical simplicity, we consider $\phi = 0$. Our objective is to determine a slow time and slow space amplitude equation. A preliminary analysis indicates that we need to consider the small detuning regime in order to have bounded solutions in both space and time. To this end, we scale δ as $\delta = \varepsilon\Delta$ where $\Delta = O(1)$. We next expand parameters E_i and C, as well as the dependent variables $Z = (E, P, D)$ in power series of ε:

$$Z = Z_c + \varepsilon Z_1 + \varepsilon^2 Z_2 + \ldots \quad (6)$$

$$E_i = E_{ic} + \varepsilon E_{i1} + \varepsilon^2 E_{i2} + \varepsilon^3 E_{i3}\ldots \quad (7)$$

$$C = C_c + \varepsilon C_1 + \varepsilon^2 C_2 + \ldots \quad (8)$$

From the evolution equations, we then obtain a sequence of linear problems for the unknown functions Z_1, $Z_2, \ldots$ We analyze each problem and apply solvability conditions

in order to have a bounded solution. These conditions require that $E_{i1} = C_1 = 0$ and $E_{i2} = \sqrt{3}C_2/2$. From now on, we define the small parameter ε using equation (8) as

$$C = C_c + \varepsilon^2\alpha \tag{9}$$

where $\alpha = 1$ or -1. From the $O(\varepsilon)$ problem, we find a real solution of the form $E_1 = A_1$, $P_1 = -A_1/8$, and $D_1 = -\sqrt{3}A_1/8$ where A_1 is an unknown real function of the slow time and slow space variables. From the $O(\varepsilon^2)$ problem, we obtain $E_2 = A_2 + i\Delta A_1 + i\nabla^2 A_1/3$, $P_2 = -A_2/8 + i\nabla^2 A_1/12$, and $D_1 = -\sqrt{3}A_2/8 + A_1^2/8$ where A_2 is a new real unknown function of the slow time and slow space variables. Since A_1 is still unknown, we consider the next problem which is $O(\varepsilon^3)$. By applying the solvability condition, we obtain the following delayed Swift-Hohenberg equation (DSHE)

$$4E_{i3} + A(\alpha - A^2) - 4A_t\left(\gamma_c^{-1} + \frac{\gamma_\perp^{-1}}{4} + \frac{3}{4}\gamma_\parallel^{-1}\right) - 4\Delta\nabla^2 A - \frac{4}{3}\nabla^4 A + 8\eta\gamma_c^{-1}(A(t-\tau) - A) = 0. \tag{10}$$

This equation can be rewritten in a more elegant form by introducing $X = \varepsilon A$, $c = \varepsilon^2\alpha$, $Y = 4\left(E_i - E_{ic} - c\frac{\sqrt{3}}{2}\right)$ and by renaming the time variable and feedback parameters as

$$t \to 4\varepsilon^2\left(\frac{1}{\gamma_c} + \frac{1}{4\gamma_\perp} + \frac{3}{4\gamma_\parallel}\right)^{-1} t, \tag{11}$$

$$\eta \to 8\eta\gamma_c^{-1}\varepsilon^2, \tau \to \varepsilon^2\left(\frac{4}{\gamma_c} + \frac{1}{\gamma_\perp} + \frac{3}{\gamma_\parallel}\right)^{-1}\tau, \tag{12}$$

$$(x, y) \to \varepsilon^{1/2}(x, y), \varepsilon\Delta \to \delta. \tag{13}$$

From equation (10), we finally obtain [63]

$$X_t = Y + X(c - X^2) + a_1\nabla^2 X + a_2\nabla^4 X + \eta(X(t-\tau) - X) \tag{14}$$

where $a_1 = -4\delta$ and $a_2 = -\frac{4}{3}$. In the next sections, we analyze this equation in detail. From now on, we shall refer to Y, X, and c as the input field, the cavity field, and the cooperative parameter, respectively. Without the delayed feedback, we recover the Swift-Hohenberg equation (SHE) derived in [66,67]. It is one of the most studied partial differential equation in various areas of nonlinear science [68–70]. It constitutes a paradigmatic evolution equation that exhibits periodic spatio-temporal patterns as well as localized structures [6,7,11,71,72].

4 Moving dissipative structures

4.1 Linear stability analysis

The homogeneous steady states solutions of the DSHE are not affected by the delayed feedback: $Y = X_s(X_s^2 - c)$. For $c < 0$ ($c > 0$) the transmitted intensity as a function of the input intensity Y^2 is monostable (bistable). A linear stability analysis of the homogeneous steady states with respect to perturbations of the form $\exp(i\mathbf{k}\cdot\mathbf{r} - \sigma\mathbf{t})$ leads to transcendental characteristic equation

$$\sigma = c - 3X_s^2 + 4\delta k^2 - \frac{4}{3}k^4 + \eta(\exp(-\sigma\tau) - 1). \tag{15}$$

The solutions of this equation show that there exist a double pair of Hopf bifurcations with a finite wavenumber or regularly called traveling wave instability, i.e., $\sigma = \pm i\Omega$. The threshold as well as the frequencies associated with these instabilities are $X_\pm = [c + 4\delta k^2 - \frac{4}{3}k^4 + \Omega\tau\tan(\Omega\tau/2)]^{(1/2)}$, and $\Omega\tau = -\eta\sin(\Omega)$. Note that the real part of the eigenvalue σ vanishes at $k = k_c = \sqrt{3\delta/2}$ which is the most unstable wavenumber at the modulational instabilities even in the absence of the delay, i.e., $\eta = 0$ and $\Omega = 0$. Under these informations, we obtain the thresholds and frequencies expressed in term of dynamical parameters

$$X_\pm = \pm\sqrt{c + 3\delta^2 + \Omega\tau\tan\left(\frac{\Omega\tau}{2}\right)}, \qquad \eta = -\frac{\sin(\Omega\tau)}{\Omega\tau}. \tag{16}$$

The corresponding thresholds for the input injected signal are $Y_\pm = (X_\pm^2 - c)X_\pm$.

The linear stability analysis is summarized in Figure 2. The time delay is fixed at $\tau = 1$. Negative values of η (feedback amplitude) can be obtained with suitable optical phase in the feedback. First, we plot the thresholds associated with a hopf instability with $k = 0$ as shown in Figure 2a. In that case, a pair of homogeneous Hopf bifurcations appears. In Figure 2b, we summarized the result obtained from a linear stability analysis in the presence of spatial coupling originated from diffraction and delay feedback. The red lines define the threshold associated with a Turing or modulational instabilities, i.e., $\Omega = 0$. For large positive values of η, the thresholds associated with the traveling waves instabilities occurs inside the red lines. For $\eta > -1$, only a Turing instability with a critical wavenumber $k_c = \sqrt{3\delta/2}$ is possible. For $\eta < -1$, we clearly see that the traveling instabilities thresholds are outside the red lines. This shows that the delay feedback affects not only the nature of the bifurcation (from Turing to traveling wave instability) but it enlarges the domain of instability. In addition, inside the instability domain, there is an infinity of instability curves. Each one is connected to a different temporal frequency with finite wave number $k = k_c$. This is exactly the critical wavenumber at the modulational instabilities obtained even in the absence of the delayed feedback, i.e., $\eta = 0$ and $\Omega = 0$. Therefore, in the framework of the Swift-Hohenberg equation, the delay feedback does not affect the wavelength of the periodic pattern that emerges from the Turing instability.

4.2 Numerical simulations

The delayed Swift-Hohenberg (14) is numerically integrated using a classical spatial finite-difference method

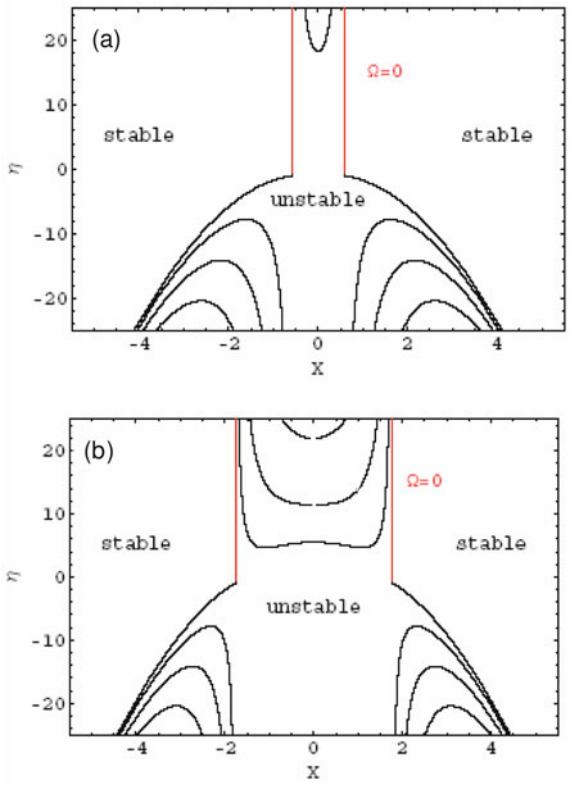

Fig. 2. (Color online) Parametric plot showing the stability boundaries associated with the Hopf instabilities. A feedback amplitude η as a function of the thresholds associated with the Hopf bifurcations $X = X_{\pm}$. (a) Homogeneous Hopf bifurcations with $k = 0$, i.e., $\nabla^2 X = \nabla^4 X = 0$; (b) inhomogeneous Hopf with $k = k_c$ (traveling wave instability). Parameters are $c = -1$, $\tau = 1$, and $\delta = 1.66$.

with forward temporal Euler integration. The boundary conditions are periodic in both transverse directions and the initial condition consists of a small amplitude noise added to the instable homogeneous steady state. We fix all the parameters except the amplitude of the injected field and the delayed feedback strength. An important property of the SHE without delay is that it has a gradient structure, i.e., admits a potential or a Lyapunov functional, and any perturbation evolves towards a stationary homogeneous or inhomogeneous distribution of light in the transverse plane. The existence of a Lyapunov functional pushes the time-evolution toward the state for which the functional has the smallest possible value compatible with the boundary conditions. However, in the presence of delay term $X(\mathbf{r}, t-\tau)$ the DSHE equation (14) loses the gradient structure. An example of the manifestation of nonvariational effect leading to the motion of periodic structures along an arbitrary direction is shown in Figure 3. Starting from a stationary light distribution in the form of hexagonal pattern obtained for $\eta = 0$, we vary the strength of the delayed feedback. For $\eta = -0.95$, the hexagonal pattern exhibits a uniform motion but keeps the hexagonal symmetry as shown in Figure 3. However, when increasing further the strength of the delayed feedback, the system

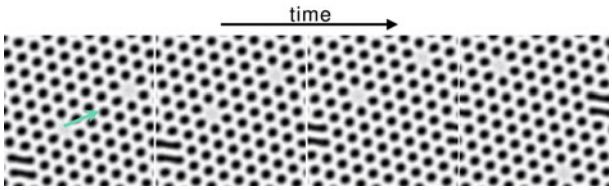

Fig. 3. (Color online) Moving hexagonal structures. Parameters are $c = 1$, $\tau = 1$, $Y = 0.2$, $\delta = 0.5$, $\eta = -0.96$. Maxima are plain white and the mesh integration is 100×100. The size of the system is 80×80. The temporal discretization used is $dt = 1/300$.

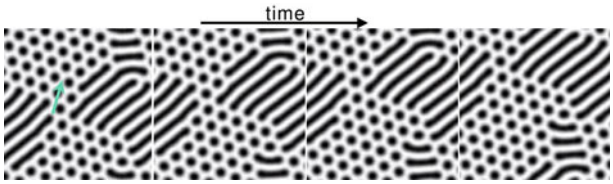

Fig. 4. (Color online) Moving 2D pattern under the effect of delayed feedback. Parameters are $c = 1$, $\tau = 1$, $Y = 0.1$, $\delta = 0.5$, $\eta = -0.96$. Maxima are plain white and the mesh integration is 100×100. The size of the system is 80×80. The temporal discretization used is $dt = 1/300$.

evolves towards a motion of stripes rather than hexagons. The delayed feedback affects the process of pattern selection when its strength exceeds some critical threshold. Another example of moving pattern in the form of stripes embedded in an hexagonal configuration is shown in Figure 4.

5 Spontaneous motion of localized dark spot

5.1 Pinning and feedback delay

Stable stationary localized structures are homoclinic solutions of equation (14) with $\partial X/\partial t = 0$. In the absence of delayed feedback, these localized structures exist in the sub-critical domain where a uniform solution and a branch of spatially periodic solution are both linearly stable [6,7,71,72]. However, in the presence of delay term $X(x, y, t-\tau)$ the DSHE equation (14) loses the gradient structure. Typical manifestation of this nonvariational effect is shown in Figure 5. When the amplitude of the delayed feedback is small, numerical simulations of equation (14) with periodic boundary conditions show that localized structures are stable and stationary i.e., $-0.95 \leq \eta \leq 0$). However, for a sufficiently large feedback strength ($\eta \leq -0.95$), a single dark localized structure exhibits a motion with a constant velocity as shown in Figure 5.

In the sub-critical domain where a uniform solution and a branch of spatially periodic solution are both linearly stable, the system exhibits high degree of multistability between structures having different number of dips. The number of dips and their spatial distribution is determined by the initial condition used. An example of moving

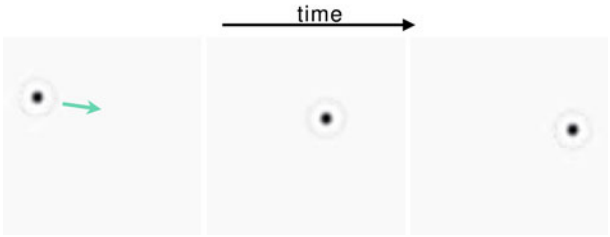

Fig. 5. (Color online) Moving single dark dissipative localized structure under the effect of delayed feedback. Parameters are $c = 1$, $\tau = 1$, $Y = 0.4$, $\delta = 0.5$, $\eta = -0.95$. Maxima are plain white and the mesh integration is 100×100. The size of the system is 80×80. The temporal discretization used is $dt = 1/300$.

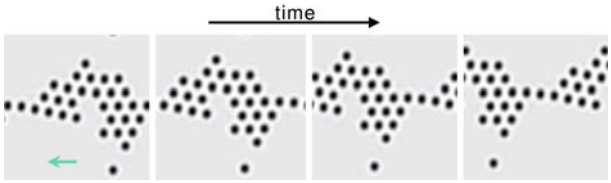

Fig. 6. (Color online) Moving cluster of dark localized structures under the effect of delayed feedback. Parameters are the same as Figure 5.

localized pattern that consists of organized clusters of dark localized spots is shown in Figure 6.

5.2 Velocity of dark localized structures

Let us now determine analytically the threshold instability associated with moving dark localized structures. To this end, we consider a radially symmetric stationary dark localized solution $X = u_0(\mathbf{r})$, $\mathbf{r} = (x\ y)^T$ of the Swift-Hohenberg equation (9). Linear stability of this solution can be analyzed by substituting $X = u_0(\mathbf{r}) + \Psi(\mathbf{r})e^{\lambda t + i\omega t}$ into equation (14) and collecting the linear in Ψ terms:

$$L\Psi = \left[\lambda + i\omega - \eta(e^{-\lambda\tau - i\omega\tau} - 1)\right]\Psi, \tag{17}$$

where the self-adjoint linear operator

$$L = c - 3X_0^2 - 4\delta\nabla^2 - \frac{4}{3}\nabla^4 \tag{18}$$

describes the stability of the solution u_0 in the absence of delayed feedback. Any eigenfunction Ψ_μ of the operator L solves equation (17) which then leads to a transcendental equation for the eigenvalue $\lambda + i\omega$ describing the stability of the solution u_0 in the presence of the feedback:

$$\mu = \lambda + i\omega - \eta(e^{-\lambda\tau - i\omega\tau} - 1), \tag{19}$$

where μ is a real eigenvalue of L corresponding to the eigenfunction Ψ_μ ($L\Psi_\mu = \mu\Psi_\mu$). Separating real and imaginary parts in (19) we get

$$\lambda = \mu + \eta[e^{-\lambda\tau}\cos(\omega\tau) - 1], \tag{20}$$

$$\omega = -\eta e^{-\lambda\tau}\sin(\omega\tau). \tag{21}$$

In what follows we assume that in the absence of the delayed feedback ($\tau = 0$) the circularly symmetric localized solution is stable, i.e., $\mu < 0$ for all the eigenfunctions Ψ_μ of the operator L, except for the translational neutral (often called Goldstone) modes given by the two components of the vector $(\Psi_x\ \Psi_y)^T = \nabla u_0$, which satisfy the relation $L\Psi_{x,y} = 0$.

The solution $u_0(\mathbf{r})$ of equation (14) with feedback term is stable when $\lambda(\mu) < 0$ for all μ belonging to the spectrum of the operator L. A bifurcation point corresponds to $\lambda(\mu)$ vanishing at some μ. Let us first consider the case when $|\eta\tau| \leq 1$. In this case the only solution of equation (21) with $\lambda = 0$ is $\omega = 0$. This solution corresponds to $\lambda = \mu = 0$ in equation (20). Hence, for $|\eta\tau| \leq 1$ the bifurcation condition $\lambda(\mu) = 0$ can be satisfied only at $\mu = 0$ which is the eigenvalue corresponding to the translational neutral modes $\Psi_{x,y}$. Next we expand equation (20) with $\mu = 0$ and equation (21) near $\lambda = \omega = 0$ up to the second order terms and solve them. This gives two eigenvalues each of them being doubly degenerate:

$$\lambda = \omega = 0, \tag{22}$$

$$\lambda = \frac{2(1+\eta\tau)}{\eta\tau^2}, \quad \omega = 0. \tag{23}$$

It follows from these equations that, at the point $\eta\tau = -1$, one has a four fold zero eigenvalue corresponding to the pair of neutral modes Ψ_x and Ψ_y. Hence, each of these eigenfunctions corresponds to a doubly degenerate zero eigenvalue that forms a 2×2 Jordan block. When the absolute value of the feedback strength is further increased $\eta\tau < -1$ two of these eigenvalues become positive and the localized solution $X = u_0(\mathbf{r})$ of equation (14) looses stability. This instability results in a drift of the localized solution.

In what follows, we compute analytically the velocity of a single peak circularly symmetric localized structure near the bifurcation point $\eta = -1/\tau$. Let us consider a deviation from the drift bifurcation point in the parameter space $\eta\tau = -1-\epsilon^2$, where ϵ is a small parameter describing the distance from the instability threshold. We look for a slowly moving localized solution of equation (14) in the form:

$$X = u_0(\xi) + \epsilon^{\mathbf{2}}\mathbf{u^{(2)}}(\xi) + \epsilon^{\mathbf{3}}\mathbf{u^{(3)}}(\xi) + \ldots, \tag{24}$$

with $\boldsymbol{\xi} = \mathbf{r} - \epsilon\mathbf{V}(\epsilon^2 t)t$. Here $\mathbf{v} = \epsilon\mathbf{V}$ is the speed of the localized solution. Substituting (24) into equation (14), using Taylor expansion

$$u_0(\boldsymbol{\xi} - \epsilon\mathbf{V}\tau) - u_0(\boldsymbol{\xi}) = -\epsilon V\tau u_1 + (\epsilon V\tau)^2 u_2/2 - (\epsilon V\tau)^3 u_3/6 + (\epsilon V\tau)^4 u_4/24 + O(\epsilon^5), \tag{25}$$

for the delayed feedback term, and collecting the third order terms in ϵ we get

$$Lu^{(3)} = \left(\frac{d\mathbf{V}}{dt}\cdot\nabla u_0\right) - Vu_1 + \frac{1}{6}\eta(V\tau)^3 u_3. \tag{26}$$

In equations (25) and (26) $V = |\mathbf{V}|$ and the coefficients u_j with $j = 1, 2, 3, 4$ are defined by $u_j(\boldsymbol{\xi}) = (\mathbf{V}\cdot\nabla u_{j-1}(\boldsymbol{\xi}))/V$.

The solvability condition for equation (26) equation requires that its right hand side be orthogonal to the translational neutral modes $\Psi_{x,y}$. Multiplying equation (26) with the linear combination of these modes $u_1(\boldsymbol{\xi}) = (\mathbf{V}\cdot\nabla u_0(\boldsymbol{\xi}))/V$ and integrating over the (x,y)-plane we obtain the equation for the localized solution velocity

$$\frac{dV}{dt} = V\left(\int_{-\infty}^{+\infty} u_1^2 d\mathbf{r} - \frac{1}{6}\eta V^2\tau^3 \int_{-\infty}^{+\infty} u_1 u_3 d\mathbf{r}\right).$$

Finally, taking into account that $\epsilon = \sqrt{-(1+\eta\tau)}$, we get the following expression for the stationary value of the soliton velocity

$$v = \epsilon V \approx \frac{Q}{\tau}\sqrt{-6(1+\eta\tau)}, \tag{27}$$

with

$$Q = \sqrt{\frac{\int_{-\infty}^{+\infty} u_1^2 d\mathbf{r}}{\int_{-\infty}^{+\infty} u_2^2 d\mathbf{r}}}. \tag{28}$$

Here we have used the relations $\int_{-\infty}^{+\infty} u_1 u_3 d\mathbf{r} = -\int_{-\infty}^{+\infty} u_2^2 d\mathbf{r}$, which is obtained using the integration by parts, and $\eta\tau = -1 + \mathcal{O}(\epsilon^2)$.

Due to the rotational symmetry of the model equation (14), the direction of the velocity $\mathbf{v}$ of a circularly symmetric localized structure is arbitrary. Therefore, the instability leading to a spontaneous motion of a moving single localized peak solution can be referred to as a circle pitchfork bifurcation [73]. Furthermore, without loss of generality the x axis can be chosen along the velocity $\mathbf{v}$. Then we obtain: $u_1 = \partial u_0(\mathbf{r})/\partial x$ and $u_2 = \partial^2 u_0(\mathbf{r})/\partial x^2$.

The constant Q in equations (27) and (28) has been evaluated numerically. For $Y = 0.25$, $c = 1$, and $\delta = 0.4$ we have obtained $Q \approx 1.33$. The soliton velocity calculated from equation (27) is in a good agreement with the velocity obtained numerically using direct numerical simulations of equation (14), see Figure 7. It is seen from this figure that near the bifurcation point $\eta\tau = -1$ the agreement is very good, while with the increase of the distance from this point the velocity calculated analytically becomes smaller than that obtained from numerical simulations. Analytical value of the threshold feedback strength $\eta_{th} = -1/\tau$ is also in agreement with that obtained numerically: $\eta_{num} = -0.96/\tau$.

6 Conclusions

We have considered a passive cavity filled by a two-level medium and driven by a coherent radiation beam in the regime of nascent optical bistability where the spatio-temporal dynamics is described by the Swift-Hohenberg equation with time delay (14). This equation supports moving periodic patterns when $\eta\tau < -1$, which depends only on the delay parameters. We showed that dark localized structures and dark localized patterns exhibit a spontaneous motion in an arbitrarily chosen direction. Finally, we have calculated analytically and numerically, the velocity of dark localized structures.

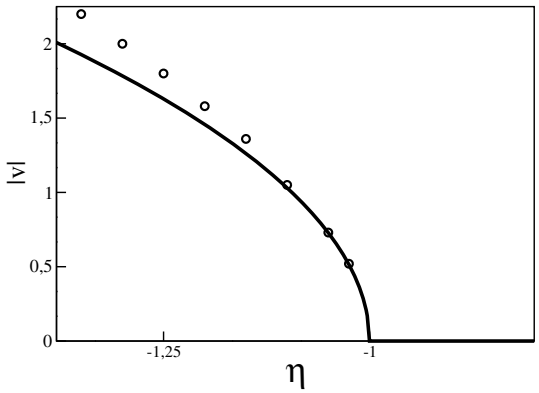

Fig. 7. Velocity of a moving dark localized structure as a function of the delayed feedback strength. Solid line indicates the velocity obtained analytically. The circles indicate the corresponding velocity obtained by numerical simulations. Same parameters as in Figure 5.

We thank P. Mandel and J.R. Tredicci for their suggestion to address this issue. This research is supported by the *Fonds de la Recherche Scientifique FRS-FNRS*, Belgium. The financial support of *Fonds Emile Defay* is also acknowledged. A.V. is supported by SFB 787 project of the DFG. This work was supported in part by the EU STREP Fun-Facs.

References

1. P. Glansdorff, I. Prigogine, *Thermodynamic Theory of Structures, Stability and Fluctuations* (Wiley, New York, 1971)
2. E. Meron, Phys. Rep. **218**, 1 (1992)
3. J. Chanu, R. Lefever, Physica A **213**, 13 (1995)
4. M.C. Cross, P.C. Hohenberg, Mod. Phys. **65**, 851 (1993)
5. R. Kapral, K. Showalter, *Chemical Waves and Patterns* (Kluwer Academic Press, Dordercht, 1995)
6. M. Tlidi, P. Mandel, R. Lefever, Phys. Rev. Lett. **73**, 640 (1994)
7. M. Tlidi, P. Mandel, Chaos Solit. Fract. **4**, 1475 (1994)
8. A.J. Scroggie et al., Chaos Solit. Fract. **4**, 1323 (1994)
9. L.A. Lugiato, M. Stefani, Europhys. Lett. **34**, 109 (1996)
10. W.J. Firth, A.J. Scroggie, Phys. Rev. Lett. **76**, 1623 (1996)
11. D.J.B. Lloyd, B. Sandstede, D. Avitabile, A.R. Champneys, SIAM J. App. Dyn. Sys. **7**, 1049 (2008)
12. V.B. Taranenko, K. Staliunas, C.O. Weiss, Phys. Rev. A **56**, 1582 (1997)
13. G. Slekys, K. Staliunas, C.O. Weiss, Opt. Commun. **149**, 113 (1998)
14. V.B. Taranenko et al., Phys. Rev. Lett. **81**, 2236 (1998)
15. V.B. Taranenko et al., Phys. Rev. A **61**, 063818 (2000)
16. S. Barland et al., Nature **419**, 699 (2002)
17. M. Pesch, E. Grosse Westhoff, T. Ackemann, W. Lange, Phys. Rev. Lett. **95**, 143906 (2005)
18. X. Hachair et al., Phys. Rev. A **72**, 013815 (2005)
19. M.G. Clerc, A. Petrossian, S. Residori, Phys. Rev. E **71**, 015205 (2005)
20. S. Residori et al., J. Opt. B Quantum Semiclass. Opt. **6**, S169 (2004)
21. S. Barbay, X. Hachair, T. Elsass, I. Sagnes, R. Kuszelewicz, Phys. Rev. Lett. **101**, 253902 (2008)

22. D. Bajoni et al., Phys. Rev. Lett. **101**, 266402 (2008)
23. P. Genevet, S. Barland, M. Giudici, J.R. Tredicce, Phys. Rev. Lett. **101**, 123905 (2009)
24. E. Caboche, S. Barland, M. Giudici, J. Tredicce, G. Tissoni, L.A. Lugiato, Phys. Rev. A **80**, 053814 (2009)
25. U. Bortolozzo, M.G. Clerc, S. Residori, New J. Phys. **11**, 093037 (2009)
26. X. Hachair, G. Tissoni, H. Thienpont, K. Panajotov, Phys. Rev. A **79**, 011801 (2009)
27. F. Haudin, R.G. Elas, R.G. Rojas, U. Bortolozzo, M.G. Clerc, S. Residori, Phys. Rev. Lett. **103**, 128003 (2009)
28. N.N. Rosanov, S.V. Fedorov, A.N. Shatsev, Phys. Rev. Lett. **95**, 053903 (2005)
29. N.A. Veretenov, N.N. Rosanov, S.V. Fedorov, J. Opt. Quant. Electron. **40**, 253 (2008)
30. C.O. Weiss, H.R. Telle, K. Staliunas, M. Brambilla, Phys. Rev. A **47**, R1616 (1993)
31. S.V. Fedorov, A.G. Vladimirov, G.V. Khodova, N.N. Rosanov, Phys. Rev. E **61**, 5814 (2000)
32. S.V. Gurevich, H.U. Bödeker, A.S. Moskalenko, A.W. Liehr, H.-G. Purwins, Physica D **199**, 115 (2004)
33. D. Turaev, M. Radziunas, A.G. Vladimirov, Phys. Rev. E **77**, 065201(R) (2008)
34. P. Coullet, J. Lega, B. Houchmanzadeh, J. Lajzerowicz, Phys. Rev. Lett. **65**, 1352 (1990)
35. D. Michaelis, U. Peschel, F. Lederer, D.V. Skryabin, W.J. Firth, Phys. Rev. E **63**, 066602 (2001)
36. K. Staliunas, V.J. Snchez-Morcillo, Phys. Rev. E **72**, 016203 (2005)
37. P.L. Ramazza et al., Phys. Rev. Lett. **81**, 4128 (2004)
38. E. Louvergneaux et al., Phys. Rev. Lett. **92**, 043901 (2004)
39. F. Papoff, R. Zambrini, Phys. Rev. Lett. **94**, 243903 (2205)
40. F. Papoff, R. Zambrini, Phys. Rev. Lett. **99**, 063907 (2007)
41. R. Zambrini, F. Papoff, Phys. Rev. E **73**, 016611 (2006)
42. K. Staliunas, V.J. Sanchez-Morcillo, Phys. Rev. A **57**, 1454 (1998)
43. L.A. Lugiato, Chaos Solit. Fract. **4**, 1251 (1994)
44. N.N. Rosanov, Progress in Optics **35**, 1 (1996)
45. N.N. Rosanov, *Spatial Hysteresis and Optical Patterns* (Springer, Berlin, 2002)
46. K. Staliunas, V.J. Sanchez-Morcillo, *Transverse Patterns in Nonlinear Optical Resonators*, Springer Tracts in Modern Physics (Springer-Verlag, Berlin Heidelberg, 2003)
47. L.A. Lugiato, IEEE J. Quantum Electron. **39**, 193 (2003)
48. Y.S. Kivshar, G.P. Agrawal, *Optical Solitons: from Fiber to Photonic Crystals* (Amsterdam, Academic Press, Elsevier Science, 2003)
49. P. Mandel, M. Tlidi, J. Opt. B Quantum Semiclass. Opt. **6**, R60 (2004)
50. B.A. Malomed, D. Mihalache, F. Wise, L. Torner, J. Opt. B Quantum Semiclass. Opt. **7**, R53 (2005)
51. N. Akhmediev, A. Ankiewicz, *Dissipative Solitons*, Series: Lecture Notes in Physics (2005), Vol. 661
52. M. Tlidi, T. Kolokolnikov, M. Taki, Focus Issue, Chaos **17**, Issue 3 (2007)
53. N. Akhmediev, A. Ankiewicz, *Dissipative Solitons: From Optics to Biology and Medicine* (Springer-Verlag, Berlin, Heidelberg, 2008)
54. T. Ackemann, W.J. Firth, G.L. Oppo, Advances in Atomic Molecular and Optical Physics **57**, 323 (2009)
55. E. Schöll, *Nonlinear Spatio-Temporal Dynamics and Chaos in Semiconductors*, Cambridge Nonlinear Science Series, No. 10 (2005)
56. T. Erneux, *Applied delay differential equations* (Sringer, 2009)
57. P.V. Paulau, D. Gomila, T. Ackemann, N.A. Loiko, W.J. Firth, Phys. Rev. E **78**, 016212 (2008)
58. Y. Tanguy, N. Radwell, T. Ackemann, R. Jager, Phys. Rev. A **78**, 023810 (2008)
59. B.Y. Rubinstein, A.A. Nepomnyashchy, A.A. Golovin, Phys. Rev. E **75**, 046213 (2007)
60. Y. Kanevsky, A.A. Nepomnyashchy, Phys. Rev. E **76**, 066305 (2007)
61. A.A. Golovin, Y. Kanevsky, A.A. Nepomnyashchy, Phys. Rev. E **79**, 046218 (2009)
62. S. Coombes, C.R. Laing, Physica D **238**, 264 (2009)
63. M. Tlidi, A.G. Vladimirov, D. Pieroux, D. Turaev, Phys. Rev. Lett. **103**, 103904 (2009)
64. T. Erneux, G. Kozyreff, M. Tlidi, Phil. Trans. R. Soc. A **368**, 483 (2010)
65. R. Lang, K. Kobayashi, IEEE J. Quantum Electron. **16**, 347 (1980)
66. P. Mandel, M. Georgiou, T. Erneux, Phys. Rev. A **47**, 4277 (1993)
67. M. Le Berre, E. Ressayre, A. Tallet, Quantum Semiclass. Opt. **7**, 1 (1995)
68. J. Swift, P.C. Hohenberg, Phys. Rev. A **15**, 319 (1977)
69. G. Kozyreff, M. Tlidi, Chaos **17**, 037103 (2007)
70. R. Lefever, N. Barbier, P. Couteron, O. Lejeune, J. Theor. Biol. **261**, 194 (2009)
71. M. Tlidi, A.G. Vladimirov, P. Mandel, IEEE J. Quant. Electron. **39**, 216 (2003)
72. G. Kozyreff, P. Assemat, S.J. Chapman, Phys. Rev. Lett. **103**, 164501 (2009)
73. M. Kness et al., Phys. Rev. A **46**, 5054 (1992)